

Solvent Effects on the Kinetics of the Dakin-West Reaction

Ayman Abdelaziz Osman^{1, 2}

¹Department of Chemistry, College of Science and Home Economic, Bisha University, Bisha, Saudi Arabia

²Department of Chemistry, College of Science and Education, University of West Kurdoan, EL Nuhud, Sudan

Email address:

aymanziz@yahoo.com

To cite this article:

Ayman Abdelaziz Osman. Solvent Effects on the Kinetics of the Dakin-West Reaction. *American Journal of Physical Chemistry*. Vol. 5, No. 6, 2016, pp. 118-127. doi: 10.11648/j.ajpc.20160506.13

Received: November 21, 2016; **Accepted:** December 5, 2016; **Published:** January 12, 2017

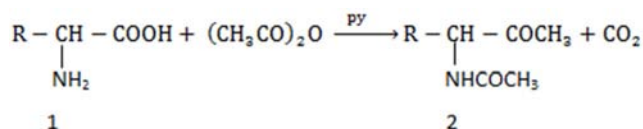
Abstract: The rate of the Dakin-West reaction have been investigated in Me₂SO, THF and CH₃CN at the temperature range (55–70) are reported. First order rate constants were obtained in each case. A Bronsted slope was found to be equal -0.0277 indicates that the transition state is very reactant-like and the proton has barely moved. Further, the solvent effect was considered from two points of mechanistic view: the thermodynamic transfer function of Me₂SO to CH₃CN and THF where the rate was found to be fast in Me₂SO and slow in THF and CH₃CN and the Kirkwood-Buff preferential solvation with aqueous Me₂SO, CH₃CN and THF. The techniques supported the proposed transition state structure.

Keywords: Dakin-West Reaction, Kirkwood-Buff Theory, Azlactone, Thermodynamic Transfer Function, Solvent Effect, Bronsted Plot, Activity Coefficient

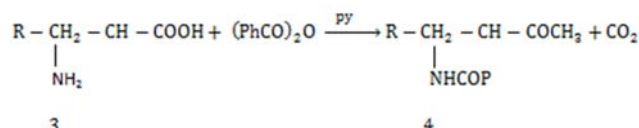
1. Introduction

1.1. The Dakin – West Reaction

The direct conversion of an α- amino acid (1) into the corresponding acetamido alkyl methyl ketone (2) by the action of acetic anhydride in the presence of pyridine, with the evolution of carbon dioxide was recognized by Dakin and West [1]



Dakin and West showed that pyridine could be replaced by alkyl pyridine or sodium acetate. On the other hand acetic anhydride may be replaced by other anhydrides affording for example ethyl- or propyl-ketones in good yields, under modified reaction condition, but, in general, yield diminishes with increasing chain length in the acid anhydride [2, 3].



Cleland and Nieman reported that benzoic anhydride gives a moderate yield of phenyl ketone [2]. But neither phthalic anhydride nor acetic anhydride products any ketone from phenyl alanine.

1.2. Mechanism of the Dakin – West Reaction

The reaction of glycine (5) with acetic anhydride in the presence of pyridine to give α-acetamido alkyl methyl ketone (14). The reaction proceeds through acylation of glycine, cyclization of acylated product to an azlactone (7) and the reaction of azlactone with pyridine to give resonance-stabilized carbanion, which reacts with acetic anhydride to give azlactone (9) of the acetamido-β-keto acid, subsequent conversion of the azlactone to the acetamido ketone (14) and carbon dioxide follows as shown in Figure 1.

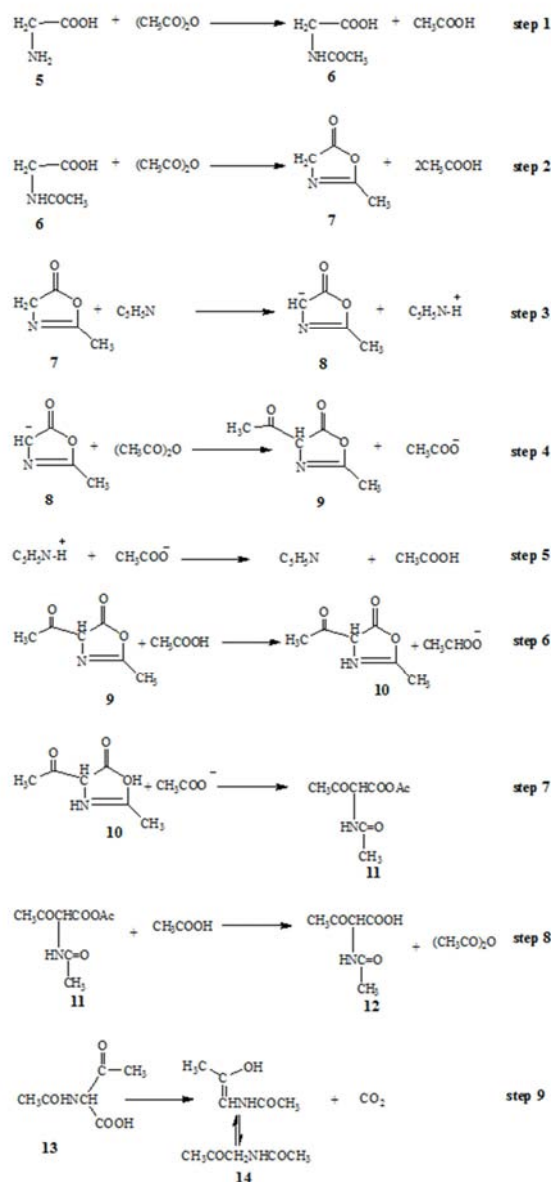


Figure 1. Mechanism of the Dakin-West Reaction.

1.3. Base Catalysis of the Dakin-West Reaction

The behavior of an acid or base on the ionization (exchange a proton with solvent) is closely related to its behavior as general acid or base catalyst (exchanging a proton with a substrate). The relationship was quantified by Bronsted and Pederson following their development of the principle of general acid and base catalysis. Their equations are expressed as:

$$\log K_a = \alpha \log K_a + C_a \quad (1)$$

$$\log K_b = \beta \log K_b + C_b \quad (2)$$

where K_a and K_b are the rate constant for the acid and base catalyzed reaction respectively and α , β and C are constant dependent on the reaction and its condition but independent of the catalyst. Bronsted coefficients equal zero ($\beta = 0$) have been taken as indicative of the transition state is very reactant

- like whereas those ($\beta = 1$) are indicative of the transition state is not reached till the proton is almost fully transferred to the catalyst (3). When the proton is just halfway from reactant to catalyst ($\beta = 0.5$) ([4, 5])

1.4. Solvent Effect on Reaction Rate

The solvent effect on reaction rate are best treated in terms of the thermodynamics of hypothetical equilibrium between reactant and transition state, i.e., in the frame of the absolute rate theory rather than collision theory [7, 8].

The specific rate of a chemical reaction depends on the standard free-energy difference between reactants and transition state. So the first step in solving the problem of the influence of a solvent on reaction rate is there for the determination of the standard chemical potential of the reactants and transition state in a various solvent.

Any consideration of solvent effect on rates or equilibria must start from solvent activity coefficient γ^s , for reactants, transition state and products. Once solvent activity coefficient are available or can be predicted, it is highly probable that enormous amount of information on the kinetics of reactions in solution and on equilibrium properties such as solubility, acid-base strength, and kinetics of reaction in the different solvent can be reduced to a relatively small number of constants [9, 10]. The solvent activity coefficient is defined as in equation (4) such that γ^s is proportional to change in the standard chemical potential, μ_i of solute 1, (hypothetically ideal in respect to Henry's law, unimolar solution), on transfer from an arbitrarily chosen reference solvent and another solvent respectively [11, 12].

Hence

$$\mu_i^s = \mu_i^\circ + RT \ln \gamma_i^s \quad (3)$$

if the transmission coefficient is unity, the rate of reaction is given by Eqn. (4).

$$\text{rate} = \frac{KT}{h} [X^\ddagger] \quad (4)$$

where k is Boltzman constant, h is planks constant.

For bimolecular reaction $A + B \rightleftharpoons [X^\ddagger] \rightarrow \text{product}$ in the solvent (s), is given by Eqn. (5).

$$[X^\ddagger] = K^\ddagger [A][B] \frac{\gamma_A^s \gamma_B^s}{\gamma_{X^\ddagger}^s} \quad (5)$$

Where K^\ddagger is the thermodynamic equilibrium constant between transition state and reactants.

Thus

$$\text{rate} = [A][B] \frac{KT}{h} K^\ddagger \frac{\gamma_A^s \gamma_B^s}{\gamma_{X^\ddagger}^s} \quad (6)$$

and the specific rate constant in a solvent (s) is given by Eqn. (7).

$$K^s = \frac{KT}{h} K^\ddagger \frac{\gamma_A^s \gamma_B^s}{\gamma_{X^\ddagger}^s} \quad (7)$$

In the standard solvent, γ^s is by definition, unity, so that

$$K^{\circ} = \frac{KT}{h} K^{\ddagger} \quad (8)$$

and rate constant in the different solvent is related by equation (9) which allows a quantitative prediction of solvent effects on rates of reactions if ${}^{\circ}\gamma_i^s$ for the solutes and solvent are known or can estimate.

$$K^s = K^{\circ} \frac{{}^{\circ}\gamma_A^s {}^{\circ}\gamma_B^s}{{}^{\circ}\gamma_{X^{\ddagger}}^s} \quad (9)$$

1.4.1. Thermodynamic Transfer Function

The thermodynamic transfer function approach of medium change is highly informative concerning transition-state structure enabling one to deduce stable effects of charge distribution and the correlation between medium effects and structure relationships. In 1960s Arnett, amid to explain the variation of the hydrolysis of tetr-butyl chloride in alcohol-water mixture and on the other with Parker's studies of bimolecular nucleophilic substitution reaction in dipolar aprotic solvents. The latter were found to have very large rate-enhancing properties in many instances as compared with hydroxylic solvents [13, 9].

The free energy change (ΔG) for the reaction on going from one solvent to another can be measured by measuring solubilities in each solvent and a third immiscible solvent because the reactant in the solvent is in equilibrium with reactant as solid or as a solution in the immiscible solvent. As a result of Parkers measurement the sum of ΔH , ΔS and ΔG for the reactants together can be found, these may then be combined with the value of, ΔH^{\ddagger} , ΔS^{\ddagger} and ΔG^{\ddagger} for the activation process to get ΔG value for the transition state by equation (10) and (11) and this is illustrated in Figure 2. [13, 14, 15].

$$-RT \ln(k_B/k_A) = \Delta G_B^{\ddagger} + \Delta G_A^{\ddagger} \quad (10)$$

$$\Delta G_B^{\ddagger} = \sum \Delta G_B^A + \Delta G_B^{\ddagger} - \Delta G_A^{\ddagger} \quad (11)$$

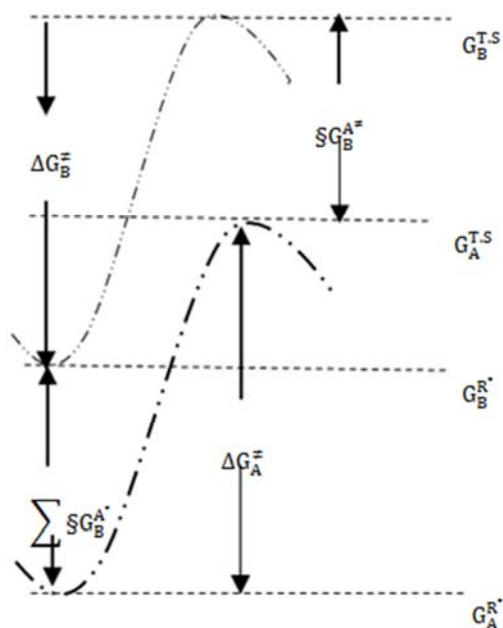


Figure 2. Calculation of the free energy of transition state from solvent A to solvent B.

ΔG_A^{\ddagger} = change in free energy of activation of solvent A.

ΔG_B^{\ddagger} = change in free energy of activation of solvent B.

$\sum \Delta G_B^A$ = change in standard free energy of transfer of a solute from solvent A to B.

ΔG_B^{\ddagger} = change in standard free energy of transfer of transition state from solvent A to B.

1.4.2. Kirkwood-Buff Treatment of Preferential Solvation

The Kirkwood-Buff treatment of liquid systems shows that the thermodynamic properties of a mixture are used to obtain information concerning spatial pair correlation function, $g_{12}(R)$, $g_{22}(R)$ and $g_{11}(R)$ where R is the scalar distance. The link between these function and thermodynamics properties through the integral function G_{11} , G_{22} and G_{12} . Thus for the integral function G_{12} [10]. It has been observed that by changing the composition of the aqueous system it is possible to control, speed up or slow down a given chemical reaction [16]. The aqueous mixture has been classifying into typically aqueous and typically nonaqueous mixtures. The mixture is classified as typically non-aqueous mixtures if excess molar enthalpies of mixing (H_m^{\ddagger}) are large than the excess molar entropies-temperature product i.e ($H_m^{\ddagger} > TS_m^{\ddagger}$). The Kirkwood-Buff treatment of liquid systems was originally aimed at showing how the thermodynamics properties of a mixture could be classified from knowledge of angle-averaged. Pair-correlations functions, $g_{12}(R)$, $g_{22}(R)$ and $g_{11}(R)$ where (R) is the scalar distance. The link between this function and the thermodynamic properties is established through the integral function G_{11} , G_{22} and G_{12} . Thus for the integral function G_{12} ,

$$G_{12} = \int [g_{12}(R) - 1] 4\pi R^2 \cdot dR \quad (12)$$

the function G_{12} measures the tendency of molecules of liquid 1 toward the molecules of liquid 2. The inverse Kirkwood-Buff developed by Ben-Naim uses the thermodynamic data of a given mixture to calculate the integral function G_{11} , G_{22} and G_{12} . For ethanol (2) and water (1), the function G_{11} , G_{22} and G_{12} have been calculated using excess molar Gibbs free energy molar volumes, and isothermal compressibilities, κ_i at 298.2 K [17]. The integral function expresses the affinity of solute j for solvent 1 in its cosphere [17, 18]. The analysis of the rates of reaction in an aqueous solvent in the whole mole fraction ranges and their comparison with molar excess thermodynamics function and Kirkwood-Buff integral functions may yield valuable mechanistic information regarding the transition state. These observations have been known to point out an interesting link extending from kinetics through equilibrium thermodynamics properties of the solution and liquid mixtures to statistical thermodynamics treatment of liquid system.

2. Method

2.1. Kinetic Measurement

Kinetic Measurement: Atypical kinetic run of the Dakin-West reaction were carried out in the following steps, the

solution of glycine (0.03 mol.dm^{-3}), pyridine (0.1 mol. dm^{-3}) and acetic anhydride ($0.625 \text{ mol.dm}^{-3}$) in Me_2SO were equilibrated in a thermostat for 10 minutes. The required volume of the substrate was transferred to the reaction flask equipped with a reflux condenser. At suitable intervals of time, 2.0 cm^3 of the reaction mixture is transferred to a conical flask (100 cm^3) containing 2.0 cm^3 of hydrochloric acid to stop the reaction by hydrolysis of acetic anhydride to acetic acid and complete the volume to the mark by double distiller water. The concentration of acetic acid at the time (t) was titrated using a standard solution of sodium hydroxide and phenolphthalein as indicator. The pseudo-first order rate constant was determined by the integrated rate law for the first-order reaction and the thermodynamic activation parameters were calculated.

2.2. Determination of Activity Coefficient

Activity coefficient was obtained from freezing point depression data for the glycine in Me_2SO and boiling point elevation for THF and CH_3CN solvent. This was done by an improved method due to Beckmann, using ordinary freezing point depression apparatus [7]. The activity was obtained from the Eqn. (13).

$$a_{\text{Me}_2\text{SO}} = \exp\left(\frac{H_{f\text{Me}_2\text{SO}} \Delta T_f}{R T_f^2}\right) \quad (13)$$

where:

T_f = Freezing point of = $12.6 = 6.527 \text{ kJ mol}^{-1}$

ΔT_f = Freezing point depression

$H_{f\text{Me}_2\text{SO}}$ = molar heat of fusion of Me_2SO = $6.527 \text{ kJ mol}^{-1}$

and the activity coefficient of the solvent dimethyl sulphoxide $\tau_{\text{Me}_2\text{SO}}$ was obtained from the equation (14).

$$\tau_{\text{Me}_2\text{SO}} = \frac{a_{\text{Me}_2\text{SO}}}{X_{\text{Me}_2\text{SO}}} \quad (14)$$

where $X_{\text{Me}_2\text{SO}}$ is the mole fraction of Me_2SO in the various solutions. Finally a plot was made of $(X_{\text{Me}_2\text{SO}}/X_{\text{gly}})$ vs $\ln \tau_{\text{Me}_2\text{SO}}$ where X_{gly} is the mole fraction of glycine in solution.

The plotted curve is extrapolated and the area under the curve is determined. The activity coefficient is given by Eqn. (15).

$$\tau_{\text{Me}_2\text{SO}} = \exp(-\text{Area}) \quad (15)$$

From the boiling point elevation data, the activity and activity coefficient was similarly calculated for CH_3CN and THF.

3. Result and Discussion

3.1. Base Catalysis of the Dakin-West Reaction

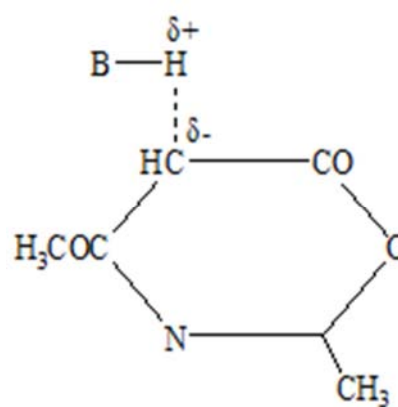
Base Catalysis on the rate of the reaction was investigated by using the series; pyridine, trimethylamine, tri-n-butylamine, aniline and *O*-nitro aniline in Me_2SO at 70. At

the rate-limiting step of the reaction is the removal of a proton from the amino acid or its azlactone derivative. It might be anticipated that the catalytic activity of the series of bases would parallel their ionization constant, generally considered as a measure of proton-accepting ability. The rate of reaction in different bases is shown in Table 1.

Table 1. The rate of reaction of glycine with acetic anhydride in various bases.

Base catalyst	K. $\text{min}^{-1} \times 10^{-3}$	Log k	pK _b
Triethylamine	59.62	-1.22	3.20
Tri-n-butylamine	56.59	-1.25	3.60
Pyridine	42.35	-1.37	8.80
Aniline	38.89	-1.41	9.40
O-nitro aniline	21.43	-1.67	13.00

It can be seen that from the table 1, the bases have a considerable effect on the reaction rate. In the series pyridine, triethylamine and tri-n-butylamine, the higher rate constant can be attributed to the greater electron availability on the nitrogen atom. It seems plausible that the slow rate of the reaction which obtained with aniline and *O*-nitro aniline is due to the most rapid formation of the conjugated base of an azlactone intermediate. This can interpret in term of proton transfer from azlactone to base in the rate-determining step. This could be due to increasing steric hindrance or increase the energy of dissolution that must precede proton transfer. This observation support that the transition state is stabilized when pyridine, triethylamine, tri-n-butylamine uses as a catalyst and destabilized in other bases. A plot of log k_o versus pK_a gave a linear relation, Figure 3, from the slope ($\beta = -0.0277$) is near zero, this indicates the transition state is very reactant-like and the proton has barely moved in the transition state. There is a negative charge very close to the catalyst and the positive charge developing in the base catalyst is delocalized away from the reaction site. From these finding a quasi-membered ring azalactone was proposed s possible transition state structure.



(7a)

King and McMillan suggested the same transition state in the reaction of *O*-chloro phenyl acetic with acetic-1-c¹⁴-anhydride in the presence of pyridine [6]

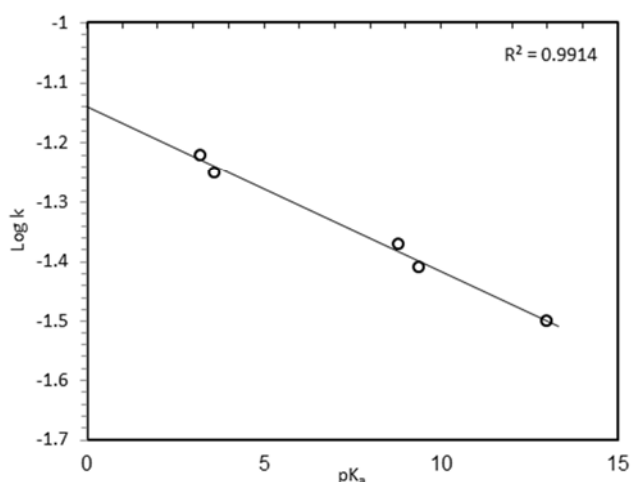


Figure 3. Bronsted dependence of $\log k_o$ vs pK_b for the reaction of glycine with acetic anhydride.

3.2. Thermodynamic Transfer Functions

Differential solvation of initial and transition state is an important tool in mechanistic studies. The solvent effects on the rate of reaction were investigated by changing the solvent from Me_2SO to CH_3CN and THF.

3.2.1. Me_2SO to THF

Table 2 records the rate constant, activity coefficient and solubility of reactant glycine with acetic anhydride in Me_2SO and THF as solvent

Table 2. The rate constant, activity coefficient and solubility of glycine in Me_2SO and THF (in mole fraction).

Parameter	Me_2SO	THF
Rate constant (k. min^{-1}) $\times 10^{-3}$	43.35	16.04
Solubility	0.59	0.36
Activity coefficient	0.17	0.12

Comparison of the rate constant in table 4 showed that the reaction in Me_2SO is faster than THF. The energy of transfer for reactant and transition state for the reaction summarized in table 3.

Table 3. Thermodynamic analysis of differential solvation at 70 from Me_2SO to THF (G , in kJ. Mole^{-1}).

$k_{\text{Me}_2\text{SO}}/k_{\text{THF}}$	+2.61
$\Delta G_{\text{THF}}^{\text{Me}_2\text{SO}^\circ}$	+1.91
$\Delta G_{\text{Me}_2\text{SO}}^\ddagger - \Delta G_{\text{THF}}^\ddagger$	+2.18
$\Delta G_{\text{THF}}^{\text{Me}_2\text{SO}^\ddagger}$	+4.09

It clearly seen that the initial state is slightly destabilized ($\Delta G_{\text{THF}}^{\text{Me}_2\text{SO}^\circ} = +1.91$) also the transition state destabilized on transfer from Me_2SO to THF ($\Delta G_{\text{THF}}^{\text{Me}_2\text{SO}^\ddagger} = +2.18$) more than initial state destabilization. The above destabilization is greater in magnitude as compared to the ground state destabilization. This is strong indication of development-charge in the transition state which is in accord with the

postulated transition state. The negative center in Me_2SO is on a less hindrance oxygen and interacts more strongly with positive centers in the transition state than does the negative oxygen of THF [9, 10]. As a result THF solvates positively charged centers poorly and decrease reaction rate. Another factor which may explain the tremendous increase in the rate of reaction in Me_2SO as compared to the THF is the fact that Me_2SO is more basic than THF.

3.2.2. Me_2SO to CH_3CN

Table 4 record the rate constant, Activity coefficient and solubility of reactant glycine with acetic anhydride in Me_2SO and CH_3CN as a solvent.

Table 4. The rate constant, Activity coefficient and solubility of glycine in Me_2SO and CH_3CN (in mole fraction).

Parameter	Me_2SO	CH_3CN
Rate constant (k. min^{-1}) $\times 10^{-3}$	43.35	12.35
Solubility	0.59	0.20
Activity coefficient	0.17	0.09

Comparison of the rate constant in table 6 showed that the rate of reaction in Me_2SO is faster than the rate of reaction in CH_3CN . The energy of transfer for reactant and transition state for the summarized in table 5.

Table 5. Thermodynamic analysis of differential solvation at from Me_2SO to CH_3CN (G , in kJ/mole).

$k_{\text{Me}_2\text{SO}}/k_{\text{CH}_3\text{CN}}$	+3.51
$\Delta G_{\text{CH}_3\text{CN}}^{\text{Me}_2\text{SO}^\circ}$	+3.86
$\Delta G_{\text{Me}_2\text{SO}}^\ddagger - \Delta G_{\text{CH}_3\text{CN}}^\ddagger$	+2.85
$\Delta G_{\text{CH}_3\text{CN}}^{\text{Me}_2\text{SO}^\ddagger}$	+6.71

Table 5 reveal that the initial state is destabilized ($\Delta G_{\text{CH}_3\text{CN}}^{\text{Me}_2\text{SO}^\circ} = +3.86$) on transfer from Me_2SO to CH_3CN . Similarly the transition state is also destabilized on this transfer ($\Delta G_{\text{CH}_3\text{CN}}^{\text{Me}_2\text{SO}^\ddagger} = +2.85 \text{ kJ/mole}$) less than initial state destabilization. These result in overall decrease in reaction rate of reaction. The factor which may explain the tremendous decrease in rate of reaction in CH_3CN as compared to Me_2SO is the fact that the negative end of CH_3CN dipole is significantly less diffuse than the positive end. As a result CH_3CN solvated positive charge well and negative charge centers poorly. This is a strong indication of negative charge-developing in the transition state which is in accord with postulated transition state (7a). Furthermore CH_3CN has a very weak basic character. Thus CH_3CN solvated not by accepting a hydrogen bond from protic donors but essentially through ion-dipole, dipole-dipole and charge dispersion interactions. Therefore the initial and transition state are destabilized and this result in an overall decrease in reaction rate. Another factor which may explain the tremendous increase in the rate of reaction in Me_2SO as compared to CH_3CN is fact that Me_2SO is more basic than CH_3CN and glycine dissociates well in Me_2SO than in CH_3CN .

3.2.3. CH₃CN to THF

Table 6. records the rate constant, activity coefficient and solubility of reactant glycine with acetic anhydride in CH₃CN and THF as a solvent.

Table 6. The rate constant, activity coefficient and solubility of glycine in CH₃CN and THF (in mole fraction).

Parameter	CH ₃ CN	THF
Rate constant (k. min ⁻¹) x 10 ⁻³	12.35	16.04
Solubility	0.20	0.36
Activity coefficient	0.09	0.12

Comparison of the rate constant in table 6 showed that the rate of reaction in THF is faster than CH₃CN. The energy of transfer for reactant and transition state for the reaction summarized in table 6. Table 6 reveals that the initial state is stabilized ($\Delta G_{\text{THF}}^{\text{CH}_3\text{CN}^\circ} = -2.50$) on transfer from CH₃CN to THF. Similarly, the transition state is also stabilized on this transfer ($\Delta G_{\text{THF}}^{\text{CH}_3\text{CN}^\ddagger} = -0.75$ kJ/mole) less than initial state stabilization. This results in an overall increase in reaction rate.

Table 7. Thermodynamic analysis of differential solvation at from CH₃CN to THF (G, in kJ/mole).

$k_{\text{CH}_3\text{CN}}/k_{\text{THF}}$	+0.77
$\Delta G_{\text{THF}}^{\text{CH}_3\text{CN}^\circ}$	-2.50
$\Delta G_{\text{CH}_3\text{CN}}^\ddagger - \Delta G_{\text{THF}}^\ddagger$	-1.80
$\Delta G_{\text{THF}}^{\text{CH}_3\text{CN}^\ddagger}$	-0.75

The stabilization of the transition state is small in magnitude as compared to the ground state which is highly stabilized. This is a strong indication of a negative charge development in the transition state which in accord with postulated transition state (7a). The factor which may explain the tremendous decrease in the rate of reaction in CH₃CN is due to the poorly solvates of positive charge in the transition state by CH₃CN as compared to the THF solvates.

3.3. Aqueous Solvent Effect

The reaction was further investigated in aqueous Me₂SO, CH₃CN and THF. The results are listed in Table 8.

3.3.1. Me₂SO-H₂O Binary System

The rate constant increase when water is added to Me₂SO reaching a maximum at $X_{\text{Me}_2\text{SO}} = 0.2$ and decrease as $X_{\text{H}_2\text{O}}$ increase in Me₂SO – H₂O mixture (Figure 4).

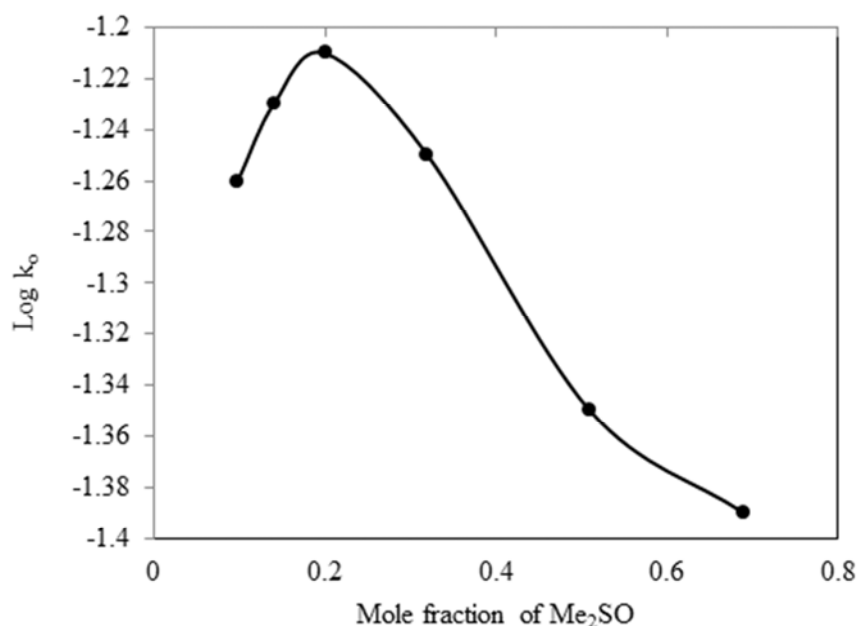


Figure 4. Variation of rate with mole fraction of aqueous Me₂SO.

The dipole-dipole interaction between Me₂SO and H₂O molecules appear to play a role increase of rate constant and evidence for this come from Raman spectra and n. m. r spectra of Me₂SO-H₂O mixture [22]. Consequently it seems as if the transition state prefers the H₂O domain to the Me₂SO domain. Therefore the postulated transition state (7a), which is charged should be highly stabilized when H₂O is added to Me₂SO and the ground state being destabilized or less stabilized than the transition state and this is observed from the increased of reaction rate. Eero also made the same observation in the acid hydrolysis of

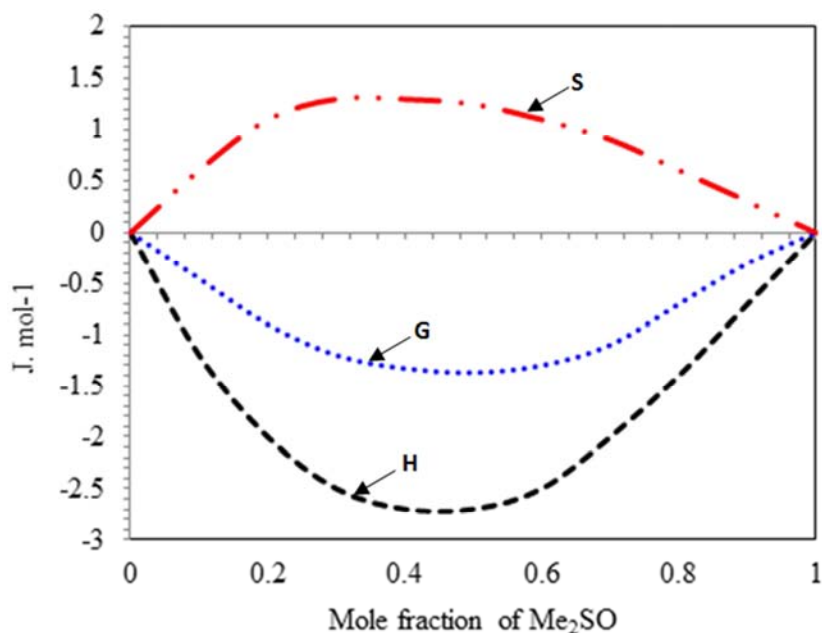
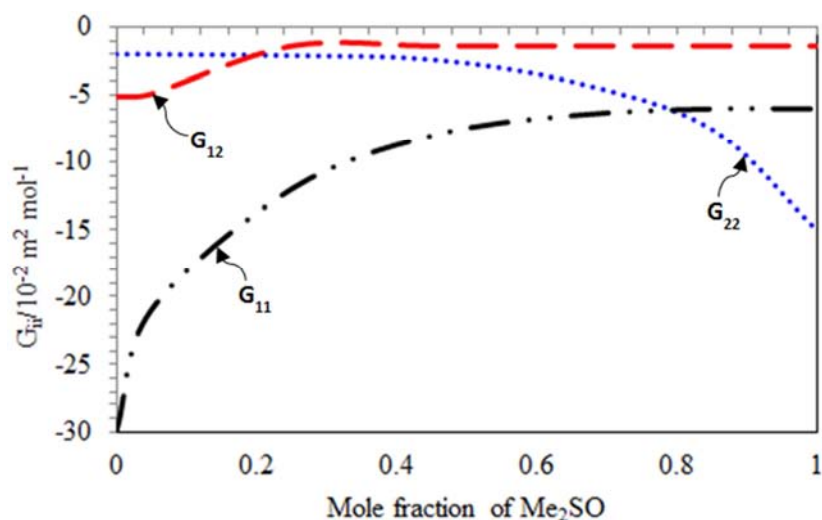
ethyl acetate in Me₂SO – H₂O mixture [19, 20]. On the other hand the ground state is destabilized as an uncharged species will prefer the Me₂SO domain to the H₂O domain [10, 21]. When water is mixed with Me₂SO much heat is evolved and the mixture becomes viscous for a short time. This may result from breakdown of Me₂SO order and formation of hydrogen bonded S=O.....H₂O which are more strongly bonded. This is responsible for the stabilization of transition state and increase in reaction rate. The interaction in Me₂SO(2)-H₂O (1) system are further

Table 8. Rate constant in aqueous Me_2SO , CH_3CN and THF.

Me ₂ SO			THF			DMF			CH ₃ CN		
Mole fraction	$K_0 \times 10^3$	Log k_0	Mole fraction	$K_0 \times 10^3$	Log k_0	Mole fraction	$K_0 \times 10^3$	Log k_0	Mole fraction	$K_0 \times 10^3$	Log k_0
0.69	40.96	-1.39	0.75	6.40	-2.19	0.68	11.28	-1.95	0.66	10.00	-2.00
0.51	45.00	-1.35	0.58	10.86	-1.96	0.48	8.55	-2.08	0.45	7.027	-2.14
0.32	56.00	-1.25	0.39	13.33	-1.88	0.30	3.00	-2.52	0.29	5.68	-2.25
0.20	61.00	-1.21	0.26	13.60	-1.87	0.19	4.69	-2.33	0.18	4.69	-2.33
0.14	58.00	-1.23	0.19	12.50	-1.90	0.14	6.25	-1.20	0.13	5.15	-2.29
0.098	55.00	-1.26	—	—	—	—	—	—	0.09	6.25	-2.20

supported by the inverse Kirkwood-Buff integrals (Figure 5). Across most of the mole fraction range, G_{12} is large than either G_{11} or G_{22} , showing no dramatic dependence on x_2 , in other word there is a strong possibility of finding water molecules and Me_2SO molecule in close proximity this consistent which strong directional hydrogen bonding

between the two components. Thus $\text{Me}_2\text{SO}(2)\text{-H}_2\text{O}(1)$ is typically non-aqueous system with both G_E^m and H_E^m being negative (Figure 6) and this is consistent with strong inter component interaction. A significant observation is that both G and H have their minima and T , S its maximum at

Figure 5. Molar Excess thermodynamic properties for $\text{Me}_2\text{SO}(2)\text{-H}_2\text{O}(1)$ mixture at [22].Figure 6. Inverse Kirkwood-Buff integral function for $\text{Me}_2\text{SO}(2)\text{-H}_2\text{O}(1)$.

3.3.2. $\text{CH}_3\text{CN}-\text{H}_2\text{O}$ Binary System

The rate constant decreased when water is added to the CH_3CN reaching a minimum at $x_{\text{CH}_3\text{CN}} = 0.18$ followed by a slight increase in reaction rate. The decrease in reaction rate could be attributed to the lack of interaction between CH_3CN and H_2O molecules. Consequently, it seems the charged transition state prefers the CH_3CN domain to the H_2O domain. Therefore the postulated transition state (7a) which is charged should be destabilized when H_2O is added to

CH_3CN and the ground state being stabilized or less destabilized than transition state. The decrease in reaction rate due to the breakdown of solvent structure of CH_3CN and formation of Structure such as $\text{CH}_3\text{C}=\text{N} \cdots \text{HOH} \cdots \text{N}=\text{CCH}_3$ which is responsible for the destabilization of the transition state and reduced reaction rate [23].

$\text{CH}_3\text{CN}(2)-\text{H}_2\text{O}(1)$ is classified as typically non-aqueous mixture positive and the excess enthalpy of $\text{CH}_3\text{CN}(2)-\text{H}_2\text{O}(1)$ is positive at low temperature (Figure 7) [25, 26].

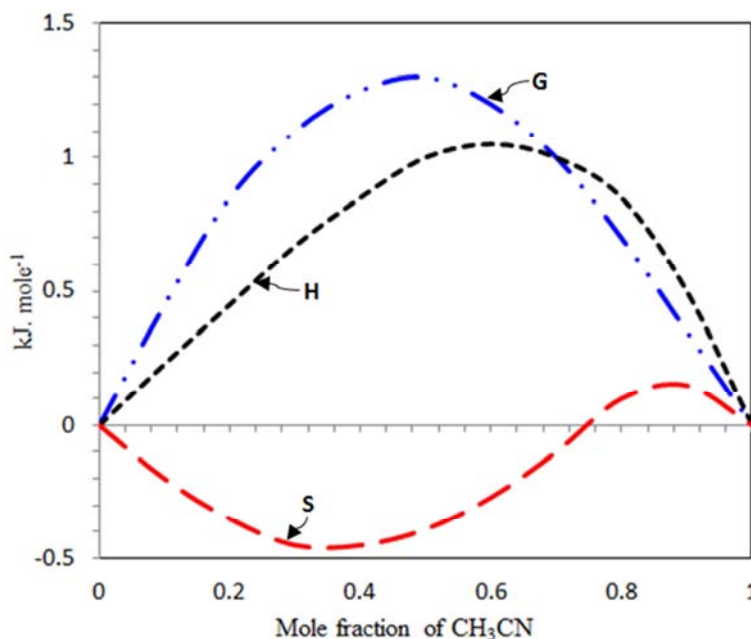


Figure 7. Molar excess thermodynamic properties for $\text{CH}_3\text{CN}(2)-\text{H}_2\text{O}(1)$ mixtures at 298 K. [22].

Evidence of this is further obtained from the Kirkwood-Buff integral function. The maxima in G_{11} and G_{12} (Figure 8) show that the probabilities of finding H_2O in close proximity to H_2O molecules and CH_3CN molecules in close proximity to CH_3CN molecules are high. On the other hand, the

minimum in G_{12} shows that the probability of finding a CH_3CN molecules near an H_2O molecule is very low. That is CH_3CN molecules cluster in CH_3CN rich domains while H_2O molecules cluster in H_2O rich domains [22].

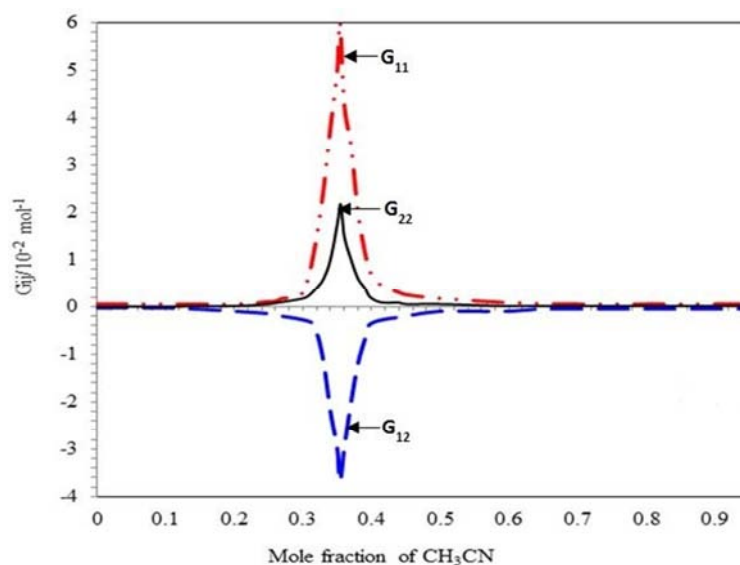


Figure 8. Inverse Kirkwood-Buff Integral Function for $\text{CH}_3\text{CN}(2)-\text{H}_2\text{O}(1)$.

3.3.3. THF-H₂O Binary System

The rate constant increases when water is added to THF rich maximum at $x_{\text{THF}} = 0.26$ and decreases as $x_{\text{H}_2\text{O}}$ than pure H₂O and THF increase. The increase in reaction rate due to a hydrogen bond between the H₂O and THF molecules is stronger [27, 28]. The increase in the rate of reaction could be explained by the fact that there is considerable interaction between THF and H₂O molecules. The increase in reaction rate on the addition of H₂O could be an indication that the transition state, which is charged, could be stabilized and ground state destabilized. Consequently, the postulated transition state (7a) charged prefers the H₂O domain to the THF domain. The increase in reaction rate in the region $0.39 > x_2 > 0.26$ seems to be simply connected with the decrease of THF content in the mixture and in this region the transition state is stabilized and ground state destabilized or less stabilized by this interaction. In the $x_{\text{THF}} > 0.19$ the rate constant decrease as increase the mole fraction of water which suggests less interaction water and THF molecules and in this region the ground state is stabilized and transition state destabilized or less stabilized resulting in reduced rate constant. Therefore the central attractive force between THF and its adjacent water further decrease the rate and enhance the water reorientation and decrease in reaction rate due to water interaction with second-nearest water neighbors are replaced by stronger Van der Waals interaction with the close THF. As more H₂O is added competition of the oxygen atom for H-bond formation leads to replacement of net-work THF-H₂O bond by water-water bond which is responsible for the observed minimum in reaction rate [29].

THF(2)-H₂O(1) is a member of typically aqueous mixture with excess function is positive is large and negative such that. The thermodynamic excess function of THF(2)-H₂O(1) are shown in (Figure 9) an interesting feature is an almost linear dependence of on over the range where the mixing change from exothermic evidently as increase to water-water hydrogen bond is replaced by water-THF hydrogen bond [10, 30].

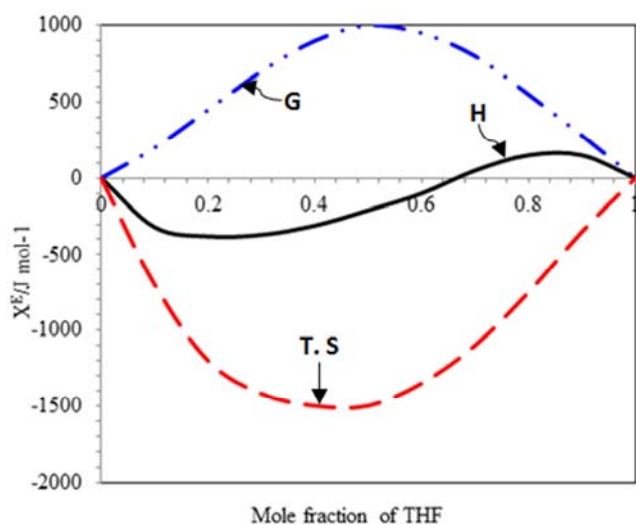


Figure 9. The excess thermodynamic function of mixing THF-H₂O mixture. [30].

4. Conclusion

From the result and discussion arising from experimental observation it is most likely that the reaction mechanism proceeds through acetylation of glycine, cyclization of acetylated product to an azalactone and the reaction of azalactone with pyridine to give resonance stabilized carbanion, followed by the rate determining step. Subsequent step are fast leading to the formation of the acetamido ketone. The Bronsted catalysis equation also in agreement with the postulated transition state structure as depicted by a slope of -0.0277 in the Bronsted plot. This is consistent and supported the transition state structure in which there is a negative charge very close to the catalyst, and the positive charge developing in the base catalyst is delocalized away from the reaction site, indicating. The transition-state is reactant – like. Thermodynamic transfer function from Me₂SO to CH₃CN ($\Delta G_{\text{CH}_3\text{CN}}^{\text{Me}_2\text{SO}^\ddagger} = +2.85 \text{ kJ/mole}$) shown that the transition state is destabilized. The destabilization of transition state on this transfer is in accord with an observation that the negative charge development in the transition state are less solvated by CH₃CN than by Me₂SO. The transition state structure is further supported by the Kirkwood-Buff treatment of preferential solution. The increase in the rate of reaction when water is added to Me₂SO could be an indication that the transition state stabilized and the ground state destabilized by this interaction. The same argument applied to CH₃CN-H₂O and THF-H₂O system has a totally a positive effect on the transition state as evidenced by the decrease rate of the reaction in addition of water to solvent molecules due to lack of interaction between solvent and H₂O molecules highly destabilized the transition state

References

- [1] N. L. Allinger, G. L. Wang, and B. B. Dewhurst. (1988) The Dakin – West Reaction. *Chem. Soc. Rev.* 17, 91-109.
- [2] G. H. Cleland and Neiman (1949). Some observation on the Dakin – West Reaction. *J. Am Chem. Soc.* 71: 841.
- [3] G. L. Buchana (1988) The Dakin –West Reaction. *Chem. Soc. Rev.* 17: 91.
- [4] R. A. Y. Jones (1979) Physical and mechanistic of organic chemistry. New York, London, p. 67.
- [5] L. P. Hammett (1940) Physical organic chemistry. McMarw – Hill Book Co., in., New York.
- [6] J. A. King and F. H. McMillan (1955) The Decarboxylative Acylation of α -substituted acid. *J. Am. Chem. Soc.* 77(10): 2814.
- [7] M. H. Abraham (1974). *Prog. Phys. Org. Chem.* 11: 2.
- [8] E. M. Arnett, W. G. Benntude, J. J. Burke (1965) Solvent Effects in Organic Chemistry. V. Molecules, Ions, and The Transition States in Aqueous Ethanol. *J. Am. Chem. Soc.* 87: 1544.

- [9] A. J. Parker (1969) Protic – dipolar aprotic solvent effect on rates of bimolecular reaction *Chem. Rev.* 9: 1.
- [10] M. J. Blandamer (1977) Kinetics solvent effect on hydrolysis of ethyl chloroformate in binary aqueous mixtures. *Adv. Phys. Org. Chem* 14: 203.
- [11] A. J. Parker (1968) *The Chemistry of Nonaqueous Solvents VA: Principles and Applications.* J. Chem. Soc. A: 220.
- [12] A. Ben-Naim (1977) Inverse of the Kirkwood-Buff theory of solution: Application to the water – ethanol system. *J. Chem. Phys.* 67: 4884.
- [13] A. J. Parker, U. Mayer, R. Schmid, and V. Gutmann (1973) *J. Org. Chem. Soc.*; 43; 1834;.
- [14] R. Elexander, A. J. Parker, J. H. Sharp and W. E. Waghorne (1972) Solvation of ions. XVI. Solvent activity coefficients of single ions. Recommended extra thermodynamic assumption. *J. Am. Chem. Soc.* 94: 1148.
- [15] B. G. Cox, A. J. Parker, *J. Am. Chem. Soc.*; 95; 408888; (1973).
- [16] R. Knorr and R. Huisgen (1970) Mechanism of the Dakin – West reaction. 1. Reaction of secondary N-acylamino acid with acetic anhydride. *Chem. Ber.* 103: 2598.
- [17] R. Knorr and R. Huisgen (1971) Mechanism of the Dakin – West reaction. 111. Course of ring opening during the Dakin – West reaction of an oxazoline – 5 olate. *Chem. Ber.* 104: 3621.
- [18] R. Knorr and G. K. Staudinger (1971) Mechanism of the Dakin –West reaction. 11. Acylation of Oxazoline – 5 –ones by carboxylic anhydride-pyridine. *Chem. Ber.* 104: 3633.
- [19] E. Tomila and M. Murto (1963) the influence of the solvent on reaction velocity, XXIV. The acid hydrolysis of ethyl acetate in dimethyl sulphoxide – water mixture. *Acta. Chem. Scand.* 17: 1943.
- [20] E. Tomila and M. Savolainen (1966) The Influence of the Solvent on Reaction Velocity. XXXI. The Reaction between Benzyl Chlorides and Methoxide Ion in Dimethyl Sulphoxide-Methanol Mixtures. *Acta. Chem. Scand.* 20: 946.
- [21] P. P. Bell (1973) the proton in Chemistry. 2 nd, ed. Chapman & Hall. London. Chapter 5: 69.
- [22] M. J. Blandamer, N. J. Blundel, J. Burgess, J. Cowles, J. Hom (1990) An inverse Kirkwood–Buff treatment of the thermodynamic properties of DMSO–water mixtures and cyano methane–water binary liquid mixtures at 298.2 K. *J. Chem. Soc. Faraday Trans.* 86(2): 277.
- [23] M. K. Chantooni and M. Kolthoff (1967) Transfer Activity Coefficients between Water and Methanol of Complexes of Some Univalent and Barium Ions with Dibenzocryptand 2.2.2, Cryptand 2.2.2, and 18-Crown-6. *J. Am. Chem. Soc.* 89: 1582.
- [24] M. K. Chantooni and M. Kolthoff (1967) Hydration of undissociated salts in acetonitrile. *J. Am. Chem. Soc.* 89: 2521.
- [25] J. D. Roberts and W. T. Moreland (1953) Electrical Effects of Substituent Groups in Saturated Systems. Reactivity's of 4-Substituted Bicyclo [2.2.2] octane-1-carboxylic Acids. *J. Am. Chem. Soc.* 75: 2167.
- [26] R. W. Taft (1952) Polar and Steric Substituent Constants for Aliphatic and o-Benzoate Groups from Rates of Esterification and Hydrolysis of Esters *J. Am. Chem. Soc.* 74: 3120.
- [27] N. Glew, H. Watts (1971) Aqueous Nonelectrolyte Solutions. Part IX. Enthalpies of Mixing of Water and Deuterium Oxide with Ethylene Oxide. *Can. J. Chem.* 49: 1830.
- [28] D. N. Glew, and N. S. Rath (1971) H₂O, HDO, and CH₃OH Infrared Spectra and Correlation with Solvent Basicity and Hydrogen Bonding. *Can. J. Chem.* 49: 837.
- [29] D. N. Glew, H. D. Mak, and N. S. Rath (1968) Aqueous nonelectrolyte solutions. Water stabilization by nonelectrolytes. *Chem. Commun.* 264.
- [30] C. Treiner (1975) Thermodynamic transfer functions for urea and thiourea from water to water-tetrahydrofuran mixtures from precise vapor-pressure measurements. *J. Chem. Phys.* 4: 471-483.